



HAL
open science

Getting from Sea to Nurseries: Considering Tidal Dynamics of Juvenile Habitat Distribution and Connectivity in a Highly Modified Estuarine Riverscape

Céline Le Pichon, Maria Alp

► **To cite this version:**

Céline Le Pichon, Maria Alp. Getting from Sea to Nurseries: Considering Tidal Dynamics of Juvenile Habitat Distribution and Connectivity in a Highly Modified Estuarine Riverscape. *Ecosystems*, inPress, 10.1007/s10021-020-00536-1 . hal-03130902

HAL Id: hal-03130902

<https://hal.science/hal-03130902>

Submitted on 3 Feb 2021

HAL is a multi-disciplinary open access archive for the deposit and dissemination of scientific research documents, whether they are published or not. The documents may come from teaching and research institutions in France or abroad, or from public or private research centers.

L'archive ouverte pluridisciplinaire **HAL**, est destinée au dépôt et à la diffusion de documents scientifiques de niveau recherche, publiés ou non, émanant des établissements d'enseignement et de recherche français ou étrangers, des laboratoires publics ou privés.

1 **Full title:**

2 **Getting from sea to nurseries: considering tidal dynamics of juvenile habitat**
3 **distribution and connectivity in a highly-modified estuarine riverscape**

4

5 **Short title:** Getting from sea to nurseries

6

7

8 **Authors :** Maria Alp^{1,2}, Céline Le Pichon¹

9

10 **Author affiliations:**

11 ¹ Université Paris-Saclay, INRAE, UR HYCAR, 1 rue Pierre-Gilles de Gennes, 92761,
12 Antony, France

13 ² INRAE, UR Riverly, 5 rue de la Doua, 69625, Villeurbanne, France

14

15 **Corresponding author:** Maria Alp, maria.alp@inrae.fr, +33 4 72 20 87 96.

16

17 **Author contributions:** MA and CLP contributed equally to study design and manuscript
18 preparation. MA led the data preparation and least-cost modelling.

19 **Abstract**

20 Productive and ecologically highly valuable ecosystems, macrotidal estuaries are also
21 characterised by complex habitat and connectivity dynamics driven by tidal and freshwater
22 influence. Organisms living in these constantly changing systems have to match their
23 movement patterns to the shifting habitat mosaic using available windows of connectivity to
24 access habitat patches of interest. This appears particularly important for the juvenile stages of
25 many fish species colonising shallow and intertidal areas of the estuaries as summer nurseries.
26 We apply tools from landscape ecology to investigate the estuarine habitat and connectivity
27 dynamics on the example of juvenile seabass (*Dicentrarchus labrax*). We test, under which
28 conditions spatio-temporal bottlenecks to estuarine nursery colonisation may emerge for this
29 species in a human-modified estuary. Combining a hydrodynamic model of the Seine estuary
30 with remote-sensing data allows us to capture structural changes in habitat availability and
31 connectivity at the estuarine scale and at a fine spatio-temporal resolution. With chronological
32 least-cost modelling of successive tidal steps, we assess patterns of nursery accessibility and
33 estimate tidal colonisation fronts for different mobility scenarios. We show that, at certain
34 hydrological conditions, tidal water level variation causes local disruptions of habitat
35 availability and connectivity, creating temporary bottlenecks for seabass juveniles'
36 movement. Fish mobility appears determinant for their vulnerability to these connectivity
37 disruptions. Our approach allows for quantitative assessment and visualisation of riverscape
38 complexity related to tidal dynamics. It is applicable to other highly dynamic ecosystems,
39 where the mobile nature of connectivity and habitats needs to be integrated into conservation
40 and management planning.

41

42 **Keywords:** least-cost modelling, spatio-temporal hydrodynamics, functional connectivity,
43 habitat patch dynamics, tidal cycle, dispersal, nursery habitats, Seine estuary, European
44 seabass *Dicentrarchus labrax*

45 **Manuscript highlights**

- 46 • Tidal estuarine habitat distribution and connectivity change on an hourly scale
- 47 • Transient bottlenecks to movement emerge in estuaries with modified topography
- 48 • Juvenile fish sensitivity to these bottlenecks depends on their swimming capacity

49 **Introduction**

50 When speaking of animal habitats in a landscape perspective, we may be inclined to imagine
51 clearly defined stable patches either isolated or connected by animal movement. In reality,
52 environmental parameters delimiting habitats and determining landscape connectivity are
53 often subject to substantial fluctuations. In dynamic ecosystems, the distribution of habitat
54 patches changes spatially over time (“shifting habitat mosaic”, Stanford and others 2005;
55 Wimberly 2006) and so does their accessibility characterised by “transient windows of
56 connectivity” (Zeigler and Fagan 2014). Several spatio-temporal scales may be involved in
57 such dynamics determined by natural or anthropogenic drivers. For instance, distribution of
58 vegetation cover (and thus of habitat patches) in a landscape may be re-set by volcano
59 eruptions or earthquakes occurring on the temporal scales of centuries or thousands of years,
60 or by more frequently recurring disturbances, such as fire or violent storms (Zeigler and
61 Fagan 2014). In river floodplains, large-scale “reshuffling” of habitat mosaic results primarily
62 from major flood events (Hohensinner and others 2011), while natural or artificial
63 fluctuations of environmental parameters (e.g. temperature or water level), occurring on the
64 daily or hourly basis, may affect habitat patch distribution and connectivity at finer spatio-
65 temporal scales (Capra and others 2017; Tonolla and others 2010).

66 Theoretical modelling has allowed to explore the drivers of metapopulation
67 persistence in dynamic mosaic landscapes (Fahrig 1992; Keymer and others 2000),
68 demonstrating the importance of matching between spatio-temporal scales of landscape
69 dynamics and the life history traits of an organism, such as its life span and dispersal capacity.
70 Animal life cycle may involve movement related to changes of vital space between life
71 stages, most evident in species with complex life cycles shifting between terrestrial and
72 aquatic, or marine and freshwater environments. Furthermore, within the vital space of each
73 life stage, daily or seasonal movements between different habitat types may also occur

74 (Figure 1). The term “connectivity fractal” has been suggested by Sheaves (2009) to describe
75 the pattern produced by « the hierarchy of migrations at a variety of scales that connect a
76 variety of habitats in complex ways”.

77 For understanding population dynamics within a landscape, it is crucial to link the
78 habitat-patch-dynamics perspective with a temporal perspective on the organism’s life history
79 including its changing dispersal capacity (Wiens 1976). This involves considering landscape
80 structure and landscape connectivity in terms of propensity or resistance to movement
81 (Baguette and others 2013; Taylor and others 1993). The landscape may thus be seen as an
82 organism- and stage-specific map of habitat patches connected by “highways”, “backroads”,
83 “barriers” etc. Furthermore, as the sequence of life cycle events occurs in a certain non-
84 random and non-reversible order, taking a chronological approach is necessary for
85 understanding “life cycle connectivity” within a given landscape.

86 Empirical studies of habitat distribution and landscape connectivity are challenging in
87 large dynamic ecosystems, as they require spatio-temporally explicit data acquired at
88 appropriate scales and a sufficiently fine resolution. Where direct observations of movement
89 are difficult, functional connectivity modelling offers a way of quantifying and predicting
90 habitat distribution and accessibility (Adriaensen and others 2003). It became particularly
91 promising in the view of technological developments in remote-sensing and environmental
92 modelling allowing for access to continuous environmental data with high resolution in space
93 and time (Carbonneau and Piégay 2012; Neumann and others 2015). When supported by good
94 knowledge of species ecology and dispersal capacity, these tools allow producing map
95 sequences of habitat patch distribution and landscape permeability for movement.

96 Habitat accessibility can then be assessed with least-cost modelling, whereby least-
97 cost paths correspond to “effective distances” between habitat patches estimated to have the
98 lowest energetic cost and a maximum potential of survival (Adriaensen and others 2003;

99 Zeller and others 2012). This approach has allowed identifying terrestrial wildlife corridors in
100 conservation context at the scales from hundreds of kilometers for large mammals (Rouget
101 and others 2006) to few hundreds of meters for amphibians (Ray and others 2002) and
102 invertebrates (Sutcliffe and others 2003). It has also been applied in riverscapes (Foubert and
103 others 2019; Hanke and others 2014) and seascapes (Caldwell and Gergel 2013), but, until
104 recently, hardly used in highly dynamic aquatic systems (but see Foubert and others 2019).

105 Macrotidal estuaries represent an ecosystem with particularly complex habitat
106 dynamics involving several temporal scales. Daily tidal dynamics interact here with seasonal
107 patterns of freshwater discharge, driving environmental variability (salinity, water level,
108 current velocity and direction) and creating high spatio-temporal habitat heterogeneity. The
109 extremes of such variation can be observed in the intertidal habitats (tidal creeks, salt
110 marshes, mudflats), transformed within hours from nearly terrestrial at low tide to aquatic at
111 high tide. These highly productive habitats are of particular ecological value, as they are an
112 important part of nurseries for many fish and invertebrate species (Bretsch and Allen 2006;
113 Rountree and Able 2007), representing functional habitats, which contribute to their feeding,
114 growth and survival at early stages and offer refuge from predators (Cattrijsse and Hampel
115 2006; Rountree and Able 2007). Importantly, spatial distribution of optimal nursery habitat
116 patches changes with the progression of the tide due to water level and flow velocity
117 fluctuations creating a true “shifting habitat mosaic” on very short temporal scales. Juveniles
118 of many marine and estuarine fish species have adapted their behaviour to the tidal cycle,
119 effectuating daily migrations to temporarily available habitats (Gibson 2003; Laffaille and
120 others 2001; Martinho and others 2008) or using strong tidal currents (selective tidal
121 transport) to advance on a larger spatial scale in a required direction (Forward and Tankersley
122 2001).

123 Many of today's estuaries have been strongly degraded by human activities (Lotze and
124 others 2006). Strategic nodes for navigation and integrators of basin-scale processes, they
125 have a long history of morphological and physico-chemical alteration: channelization,
126 shoreline armoring, as well as upstream-derived impacts such as pollution, changes of river
127 flow regime, or sediment transport. This could have several effects on the habitat dynamics in
128 the estuarine intertidal zones. First, habitat patch availability may be reduced through
129 modification of estuarine morphology either throughout the tidal cycle or at its specific steps.
130 Second, connectivity between available habitat patches might be temporarily disrupted during
131 the tidal cycle, impeding the organisms, which colonise them, to complete their tidal
132 migration cycle.

133 The objective of our work was to quantify fish habitat availability and accessibility in
134 a macrotidal human-impacted estuary using a chronological map-based modelling approach.
135 We applied tools from functional landscape modelling developed for riverscapes (Roy and Le
136 Pichon 2017) to the case of tidal migration of juvenile European seabass (*Dicentrarchus*
137 *labrax*) towards summer nurseries of the Seine estuary at the moment of their colonisation.
138 Our study organism is a marine species with a well-documented life-cycle and extensive
139 experimental evidence on swimming capacity at different stages. Specific questions we asked
140 for seabass were: i) How do water level fluctuations affect the extent and distribution of its
141 estuarine nursery habitats? ii) Does a morphologically modified estuary allow for a
142 continuous functional connectivity of the nursery habitats on a large scale and thus for their
143 colonisation by early juveniles?

144 To address these questions, we considered two temporal scales of variation and
145 conducted both an intra-annual and an intra-tidal analysis. We first tested for the effects of a
146 range of tidal coefficients (TC) and two discharge levels on seabass nursery availability at
147 high tide. Then, for two contrasted cases of hydrological conditions, we quantified nursery

148 and ebb habitat availability at different steps of the tidal cycle and modelled initial
149 colonisation of these habitats by seabass juveniles. Throughout the paper we used the term
150 “estuarine colonisation” to designate the process of first access of young juveniles from the
151 estuarine mouth to the whole extent of estuarine nurseries up to the upstream limit of their
152 salinity preferences. This large-scale and potentially multi-step advancement profits from
153 selective tidal transport during the flood stages of the tidal cycles. “Estuarine colonisation”
154 results in the establishment of juveniles in certain areas of the estuary, where they were not
155 initially present, and where they can then enter daily cycles of moving between patches of
156 habitat available at different moments of the tide, or “tidal migrations” (Rountree and Able
157 2007, Sheaves 2009).

158

159 **Materials and Methods**

160 **Study site**

161 The Seine estuary (Figure 2) is an example of a large macrotidal estuary of the European
162 Atlantic coast highly modified by human activities (Tecchio and others 2016). It is
163 characterised by a semidiurnal regime and tidal amplitude of 8.5 m in the mouth area (Lafite
164 and Romaña 2001). The spatial extent of tidal waters covers 170 km of river length, and is
165 limited by the Poses dam upstream. The mean annual Seine river discharge measured at Poses
166 is $450 \text{ m}^3 \text{ s}^{-1}$ (50 to $2200 \text{ m}^3 \text{ s}^{-1}$).

167 Originally, the mouth of the Seine estuary was a large and shallow braided system
168 characterised by islands, mobile sandbanks, and extensive intertidal areas with mudflats and
169 salt marshes (Avoine and others 1981; Lesourd and others 2016; Figure 2), while the
170 upstream freshwater part was a meandering river with numerous islands, shoals and pools.
171 Since 1834, the Seine estuary has been experiencing morphological and sedimentary

172 modifications to secure boat traffic and stabilise river flow through channel containment,
173 dredging, diking and island removal. Furthermore, the Normandy Bridge construction (1995),
174 and the new port extension of Le Havre (2006) have considerably modified the structural
175 aspects and the hydrodynamic conditions at the Seine estuary, causing further loss of
176 intertidal habitats. Separating the main channel from the riverbanks by submersible dikes has
177 narrowed the estuary (Grasso and Le Hir 2019) and restricted its lateral connectivity.
178 Altogether, the estuary has lost 78% of its intertidal areas and 80% of the islands since the
179 beginning of the 20th century (Lafite and Romaña 2001; Cuvilliez and others 2009), with
180 76% of banks in the estuarine mouth being diked (Foussard and others 2010). The nursery
181 capacity of the Seine estuary has been strongly affected by these changes, for instance, for
182 flatfish, it has been estimated to be reduced by 42% (Rochette and others 2010).

183 Study species

184 European seabass (*Dicentrarchus labrax*) is a highly exploited fish species of the North East
185 Atlantic (NEA) coast, whose northern stock has been declining over recent years (López and
186 others 2015). The life cycle of NEA populations takes place between marine, coastal and
187 brackish habitats. Seabass spawn offshore in early spring with post-larvae spending about a
188 month in the unstratified waters of the English Channel (Jennings and Pawson 1992). Nursery
189 settlement at the NEA coast occurs between April and September, about 2-3 months upon
190 hatching, followed by the metamorphosis into juveniles between 50 and 110 days post-hatch
191 (Jennings and Pawson 1992; López and others 2015). In spring, once the water temperatures
192 increase, assisted by tidal currents, seabass juveniles colonise coastal and estuarine nurseries
193 and start daily migrations between subtidal and intertidal habitats in poly- and mesohalin
194 zones (Jennings and Pawson 1992; Cabral and Costa 2001). A high local site fidelity has been
195 observed, with juveniles staying for longer periods in proximity of the same nursery areas

196 (Green and others 2012). The tidal migrations continue until the onset of cold temperatures in
197 the fall, when the juveniles move to deeper areas of the estuary or to coastal habitats (Kelley
198 1986). Young seabass spend the first 2-4 years of their life in close association with the
199 estuaries, after which they shift to living in marine and coastal environments (López and
200 others 2015).

201 First-year juveniles of seabass start tidal migrations at the size of 10-15 mm (Jennings
202 and others 1991) and reach about 60 mm at the end of their first summer (Kelley 2002).

203 Dispersal capacity of early stages is rather low (with expected *in situ* swimming speeds of
204 about 0.03-0.13 m s⁻¹ for fish under 30 mm; Leis and others 2012). As many marine and
205 catadromous species, juveniles of seabass appear to have the capacity of using selective tidal
206 transport and are guided by environmental cues, such as temperature and low salinity (Pickett
207 and Pawson 1994; López and others 2015). The latter facilitate and orient their movement
208 towards the nurseries located in tidal estuaries and coastal salt marshes or mangroves
209 (Jennings and Pawson 1992). Transport with tidal currents may thus be assumed as the
210 predominant mechanism for estuarine colonisation, but it may be complemented by small-
211 scale movement in shallow areas along the shores or by using back eddies or other slack water
212 to avoid strong currents in the channel (Pickett and Pawson 1994). Furthermore, vertical
213 position selection in the water column presumably facilitating the adjustment of their
214 movement to flow velocity patterns has been reported for seabass larvae and juveniles (López
215 and others 2015). Own swimming capacity of juveniles increases rapidly with growth and
216 reaches about 0.3-0.6 m s⁻¹ by the end of the first year. Optimal speeds for late juveniles are
217 predicted at temperatures between 7 and 22°C; Claireaux and others 2006).

218 The highest abundances of seabass juveniles are found in the euhaline and mesohaline
219 zones (Selleslagh and Amara 2008). Shallow (< 2 m deep), turbid and muddy habitats typical
220 of mudflats, salt marshes and tidal creeks have been described as rich feeding grounds

221 particularly prone to becoming seabass nursery habitats (Cabral and Costa 2001; Cattrijsse
222 and others 1994) and recent stable isotope data confirm an important contribution of intertidal
223 zones to their diet (Day & Brind'Amour, unpublished data for the Seine estuary). Field
224 observations indicate that most of the seabass tidal feeding occurs during the flood and the
225 high tide (Laffaille and others 2001). Nearly no quantitative information exists on their
226 behaviour during the ebb and the low tide. During these tidal phases they have been observed
227 to stay in the areas of low flow velocities in proximity to the high-tide nurseries (personal
228 communications E.Feunteun, S.Duhamel), with some individuals remaining in warm tidal
229 pools isolated from the main stream during low tide (Pickett and Pawson 1994; Kelley 1986).
230 In the Seine estuary, this behaviour has also been reported in the intertidal areas behind the
231 dikes (pers. communication E.Feunteun). However, as this behavioural strategy involves
232 substantial risks (desiccation, exposure to predators), we may expect only a very minor
233 fraction of the population to use it.

234

235 GIS-based analysis

236 *Water depth and habitat mapping*

237 Based on temperature and discharge time series at the estuarine mouth (Online Resource 1),
238 we identified the period between April 1st and November 15th as the main period of nursery
239 use. This corresponds to the time window following the first spring river floods and when
240 temperature exceeds +10°C (a physiological threshold of feeding activity; Pastoureaud 1991).
241 For the intra-annual comparison of habitat distribution, we used ranking analysis and selected
242 two discharge levels and four tidal coefficients (TC) covering the variability of hydrological
243 conditions occurring during the time window considered: 250 m³ s⁻¹ and 800 m³ s⁻¹ exceeded
244 60% and 5% of time respectively, and TC 45, TC 65, TC 80 and TC 115 exceeded 85%, 60%,
245 35% and 2% of time respectively. Tidal coefficients as high as 115 occurred during extreme

246 spring and fall tides, while variation in tidal coefficients in the summer was well covered by
247 the range between TC 45 and TC 85 (Supplementary Figure S1c).

248 High tide water levels across the estuary were estimated statistically using a model
249 based on the interpolation of tidal heights at eighteen gauges distributed over the estuary
250 between Honfleur and Poses. For the intra-tidal analysis, a 3D-hydrodynamic model of the
251 Seine estuary was used to calculate water level, current velocity and salinity for a
252 hydrologically average year (2010; Supplementary Figure S1b) at a time step of 15 min
253 (MARS-3D; Le Hir and Lafite 2012). We expected habitat surface decrease to be the major
254 driver of fragmentation and connectivity disruption. We thus selected one discharge level
255 ($250 \text{ m}^3 \text{ s}^{-1}$) and two tidal coefficients (TC 52 and TC 85) observed in combination in 2010 to
256 cover hydrological conditions resulting in most contrasting patterns of high tide habitat
257 distribution, and achieve the closest possible match to the intra-annual analysis.

258 A regular square grid with each cell covering 5 m x 5 m, was chosen for all GIS-based
259 analyses as a compromise between i) the precision of habitat patch and barrier (e.g.
260 submersible dikes) representation and ii) the calculation time necessary for least-cost
261 modelling. For both intra-annual and intra-tidal analyses, maps of water depths were produced
262 for each discharge level–TC combination and for each considered tidal step based on the
263 difference between the estimated water level and LIDAR-based topo-bathymetric data (GIP
264 Seine Aval) for each cell of the grid.

265 In the following, when referring to the intra-tidal analysis, we use the term “tidal time
266 point” (t_N) to delimit a specific point (“snapshot”) of environmental conditions in time, while
267 “tidal time step” corresponds to the conditions in the interval (t_N-t_{N+1}) between two
268 subsequent tidal time points. Flood thus starts at t_1 (0 min) and ends with t_{14} (195 min), high
269 tide occurs between t_{14} and t_{24} (345 min) and the ebb between t_{24} and t_{49} (720 min)
270 (Supplementary Figure S2). To capture key tidal changes of habitat availability and

271 connectivity, the flood and the ebb were divided into five time steps each (e.g. t_1 - t_5 , t_5 - t_7 etc.)
272 based on two criteria: the degree of estuarine dike submergence (Figure 2) and the degree of
273 tidal creek inundation along the upstream-downstream gradient (see insets in Figure 3).

274 The spatial extent considered for this study was determined by the area with the mean
275 salinity above 0.5‰ over the tidal cycle at median TC (70). In the NEA estuaries, the post-
276 larvae have been reported to arrive to coastal areas early in spring and spend at least 30 days
277 in the proximity of the estuaries before colonising them (Jennings and Pawson, 1992). Basing
278 upon expert opinion, we assumed that in spring, early juveniles occupy moderately shallow
279 areas of the mouth of the Seine before entering the tidal cycle to access intertidal nurseries for
280 the first time (personal communication S.Duhamel). The departure habitat for colonisation
281 modelling was thus defined as estuarine mouth areas with 0.2-5 m depth (at low tide) and a
282 minimal patch size of 10 ha (Supplementary Figure S3). Tidal seabass nurseries were defined
283 as shallow areas (0.2-2 m at each time step of the flood) with either sandy or muddy substrate
284 (Fritsch 2005). Their distribution was estimated by intersecting maps of dominant (>50%)
285 bottom substrates in subtidal and intertidal areas (Online Resource 2) with water depth maps.
286 Having limited information on the low tide habitat selection, we chose a simple definition as
287 shallow areas (0.2-2 m) with current velocities not exceeding maximum juvenile swimming
288 capacity tested ($< 0.3 \text{ m s}^{-1}$) corresponding functionally to “refuge habitats”. The spatial
289 resolution of our data did not allow us to consider temporary tidal pools as potential refuge
290 habitats.

291 A value of 100 m² was chosen as a minimal patch size, smaller elements being
292 visually identified as geomatic artefacts. For the intra-annual analysis, only high-tide nursery
293 habitats were mapped, while for the intra-tidal analysis, both nursery and refuge habitats were
294 mapped at five time points of the flood (t_5 , t_7 , t_9 , t_{11} , t_{14}) and ebb (t_{27} , t_{30} , t_{34} , t_{39} , t_{45}). To
295 compare habitat distribution along the longitudinal (upstream–downstream) and horizontal

296 (north-south) axes of the estuary, we distinguished between six sectors: the estuarine mouth,
297 the area with tidal creeks, and the upstream channel located either to the north or to the south
298 of the main channel (see Online Resource 3 for a map).

299 *Resistance mapping*

300 We assumed that key factors driving estuarine permeability for the movement of early seabass
301 juveniles were current velocities in the areas submerged at each tidal time step. Resistance
302 values were assigned to each map pixel based on the current velocities. The current could thus
303 i) be neutral to movement ($R=1$); ii) facilitate movement ($R<1$); iii) impede movement ($R>1$);
304 or iv) be so high as to be avoided by the juveniles and thus considered in the model as an
305 impassable barrier ($R=10\ 000$).

306 As our connectivity model described below necessitates 2D-maps of riverscape
307 resistance to movement, flow velocities from MARS-3D model in subtidal zones were
308 averaged over the water column and across each time step. The choice of taking the average
309 value was a compromise allowing to both not underestimate the transport capacity of the tide
310 and to dampen the potential barrier effects in the most fast-flowing areas potentially avoided
311 by the juveniles through adjustment of their vertical position in the water column. Average
312 flow velocities per grid cell were divided into 6 classes. The mean of each class V_x (0.05, 0.2,
313 0.5, 0.85, 1.1, $> 1.2\text{ m s}^{-1}$) was used for the calculation of resistance values. In the intertidal
314 areas (mudflats, tidal creeks), mean flow velocities were estimated for each tidal time step
315 based on earlier field measurements (Online Resource 2). Current velocities below 0.05 m s^{-1}
316 were assumed neutral for movement. Velocities between 0.05 and 1.2 m s^{-1} were assumed to
317 facilitate movement, and resistance values R_x were calculated as inversely proportional to
318 0.05 m s^{-1} (considered equivalent to neutral to movement) ($R_x = V_x / 0.05$). We assumed that
319 flow velocities above 1.2 m s^{-1} (the fourfold of the average juvenile's own speed in their first
320 summer) would be avoided by the juveniles (due to potential risk of mortality or impingement

321 by the flow) and considered them in the model as barriers ($R=10\ 000$). Dikes, unless
322 submerged by at least 0.2 m, were mapped as pixels out of water. Based on these principles,
323 resistance maps were produced for each tidal time step (Figure 3).

324 *Least-cost modelling of habitat connectivity during the tide: a chronological approach*

325 We used ANAQUALAND (Le Pichon and others 2006) and ARCGIS 10.3 to estimate estuarine
326 mouth connectivity to seabass nursery and refuge habitats across the estuary over the tidal
327 cycle. ANAQUALAND requires 2D-raster maps of habitat patches and riverscape resistance to
328 movement as input, and takes into consideration an upstream-downstream (or vice-versa)
329 orientation of the flow direction. The software uses least-cost modelling to calculate
330 minimum functional distance to the nearest habitat patch for each pixel of the map. To
331 distinguish between pixels connected or not connected to a habitat of interest at a given point
332 in time, we applied a swimming-speed-dependent threshold value or “mobility coefficient”
333 (Roy and Le Pichon 2017) which varied depending on the tested scenario (see below). Least-
334 cost modelling of tidal flood phase was carried out for all scenarios. Furthermore, for the
335 lowest swimming speed scenario (see below), several complete tidal cycles were modelled.
336 We used a chronological principle: starting from departure patches at low tide, connectivity
337 between habitat patches was modelled over successive time steps (see Online Resource 4 for
338 details). Only habitat patches connected to the previous step (t_N) of the tidal cycle were taken
339 into account for modelling each subsequent time step (t_{N+1}) (Figure 4). During the high tide
340 (t_{14} - t_{24}), we assumed a multidirectional small-scale exploratory movement between
341 neighbouring nursery patches driven by feeding behaviour rather than further directed
342 colonisation of the estuary in its longitudinal extent.

343 A sensitivity analysis was conducted to cover several levels of mobility between early
344 spring juveniles with very weak swimming capacities ($0.05\ \text{m s}^{-1}$) and summer juveniles of up
345 to 6 cm total length progressively acquiring swimming speed. The expected sustained

346 swimming speed of the juveniles at the end of the first summer was calculated as a fivefold of
347 their body length per second ($0.6 \times 5 = 0.3 \text{ m s}^{-1}$; Leis and others 2012) and was in line with the
348 ranges of optimal speeds reported for late juveniles (Claireaux and others 2006). We modelled
349 four scenarios corresponding to four swimming speeds (0.05; 0.1; 0.2; 0.3 m s^{-1}). The
350 colonisation front for each scenario was determined as the position of the most-upstream
351 nursery habitats accessible at the beginning of the high tide.

352 To estimate the duration of complete colonisation of the estuary by early juveniles, we
353 modelled successive tidal cycles including ebb and low tide phases for the 0.05 m s^{-1} scenario
354 (at both TC 52 and TC 85), until the upstream limit of the study area was reached. Starting
355 from the second tidal cycle, the refuge habitat patches accessible at the end of the previous
356 tidal cycle were used as the departure habitat of the following tide. The low tide could
357 potentially be used for further advancing the colonisation front, if the individuals restarted
358 directed movement in the upstream direction already at this tidal stage. However: i) the actual
359 behaviour of the juveniles at low tide is largely unknown; ii) the current velocities at this tidal
360 phase are very low and multidirectional; iii) the own swimming speed of the juveniles tested
361 in this scenario was very low (0.05 m s^{-1}) and would allow them to advance in areas with no
362 assisting flow at most by 450 m over the low tide duration (2.5 h). Considering these
363 uncertainties, we chose not to take potential low-tide movement into account, and assumed in
364 the model, that the position of the juveniles in the beginning of the next flood would be
365 approximately the same as in the end of the preceding ebb.

366

367

368 **Results**

369 Intra-annual analysis: potential nursery availability at high tide

370 Our comparison of high-tide habitat distribution across different hydrological conditions
371 showed two main trends: i) a non-linear response of potential nursery surfaces to tidal
372 coefficient gradient on both north and south sides (Figure 5a), and ii) consistent differences in
373 habitat distribution between estuarine sectors (Figure 5b). The total area of potential estuarine
374 nursery surface at high tide varied by about 80 ha across the hydrological conditions tested.
375 The extremes of potential nursery surface were found at the higher discharge level ($800 \text{ m}^3 \text{ s}^{-1}$)
376 with the minimum of 351.3 ha at TC 115 (the highest TC tested) and the maximum of
377 434.4 ha at TC 45 (the lowest TC tested).

378 Under all hydrological conditions, potential habitats were predominantly located in the
379 estuarine mouth area (52-70% on the north side, and 54-87% in the south) with the rest
380 distributed between the tidal creek sector and the intertidal zones along the channel
381 (Figure 5b). Potential habitat availability in different sectors on the north side was rather
382 stable across different hydrological conditions: it varied moderately in the mouth area, and, at
383 both discharge levels, showed a progressive increase in tidal creeks and a decrease in the
384 intertidal zones along the channel with augmenting TC (Figure 5b). On the south side, the
385 relative distribution of high-tide nurseries between the mouth area and other sectors was less
386 balanced in space and time. For instance, the surface of potential nursery habitats in the
387 mouth area decreased by over 100 ha between the lowest and the highest TC (Figure 5b).
388 Nursery availability in other sectors was considerably lower on the south side compared to the
389 north side. Only in tidal creeks did it increase along the tested TC gradient with nursery
390 surface multiplied by four between the lowest and the highest TC at both discharge levels
391 (Figure 5b).

392

393 Intra-tidal analysis: dynamics of potential nursery availability

394 We found an even higher level of variation in potential nursery availability when zooming
395 into the dynamics of a single tidal cycle. During the tide, the distribution of potential nursery
396 habitats progressively shifted in the lateral and longitudinal direction resulting in no overlap
397 between the low-tide and the high-tide habitat patches (Figure 6). In the beginning of the
398 flow, most habitat patches were located in the downstream areas of the subtidal zone. With
399 the tidal water level rise, intertidal zones became progressively submerged and hydrologically
400 reconnected to the main channel, whereas some nursery patches in the mouth area became
401 unfavorable. This resulted in an unbalanced distribution of low-tide versus high-tide habitats
402 at the estuarine scale with high-tide “desert areas” (stretches completely lacking habitat)
403 emerging along the diked channel both on the south (downstream part) and the north (first
404 loop of the Seine) side (Figure 6).

405 The intra-tidal decrease of the habitat surface in the mouth area was particularly
406 pronounced in the south: habitat surface available there was four to nine times lower (at
407 TC 52 and TC 85 respectively) at high tide compared to low tide (Figure 7b). This decrease
408 was moderate in the north, where low-to-high-tide relation of habitat surface was 2:1 at both
409 TCs. Temporary loss of habitat in the mouth area was compensated by a substantial increase
410 of habitat surface in the tidal creek area (1:4 at TC 52 and 1:8 at TC 85) in the north, but not
411 in the south, where very little intertidal habitat was available throughout the tidal cycle at both
412 tidal coefficients (Figure 7b).

413 Tidal coefficient also affected the lateral habitat distribution and degree of
414 fragmentation. At TC 52, the lateral extent of habitats was smaller and the strips of habitat
415 patches along the diked channel upstream were more continuous, whereas, at TC 85, many of

416 these patches became very narrow or completely unavailable due to a drastic water depth
417 increase in this area (insets in Figure 6).

418 Connectivity analysis: nursery accessibility from the estuarine mouth

419 Both tidal coefficients and fish swimming speeds tested had a strong effect on the
420 colonisation front reached within a single flood (Figure 8). Advancement in the estuary was
421 faster at the lower tidal coefficient (TC 52). With a minimal own speed of 0.05 m s^{-1} , using
422 the upstream-directed current, the juveniles would reach the areas above the largest tidal creek
423 on the north side within a single tide (Figure 8a). Increasing swimming capacity advanced
424 their colonisation front progressively on both the north and the south side, with an average
425 gain of 9.4 km (along the shoreline) with every 0.1 m s^{-1} of own speed added. The swimming
426 speed of 0.3 m s^{-1} resulted sufficient for colonising the whole estuary within a single flood.

427 At the higher tidal coefficient (TC 85), not only did the colonisation front advance
428 substantially slower compared to TC 52 in each of the swimming speed scenarios, but also the
429 extent of this difference varied depending on the side of the estuary. Thus, while on the north
430 side, the colonisation front of the 0.05 m s^{-1} was situated 3.4 km further downstream
431 compared to the same scenario at TC 52, on the south side, this gap was about three times
432 larger (Figure 8). It is only for the swimming speed of 0.2 m s^{-1} , that colonisation fronts at TC
433 85 became approximately aligned between the north and the south side (Figure 8b). Finally, at
434 TC 85, the full extent of the estuary could not be colonised within a single tidal cycle in the
435 0.3 m s^{-1} scenario: 1.8 km and 3.7 km remained until the upstream limit of the study area on
436 the north and south side respectively.

437 Importantly, while increasing juvenile swimming speed accelerated upstream
438 advancement of the colonisation front, the effective gain in total accessible habitat surface
439 was very moderate. The number of habitat patches reached at high tide was multiplied by two

440 (TC 52) and four (TC 85) between the lowest and the highest swimming speed scenarios, but
441 this corresponded to only 30 % increase of the total habitat surface accessible across the
442 estuary (Supplementary Figure S4). This result was consistent with the general pattern of
443 habitat fragmentation along the estuary with large habitat patches available in the mouth area
444 and a high number of smaller habitat patches present in the upstream areas (Figure 6).

445 A facilitating effect of the lower tidal coefficient on the estuarine colonisation became
446 particularly evident when modelling progressive colonisation of the estuary at the lowest
447 swimming speed (0.05 m s^{-1}). The full colonisation of the estuary necessitated five tidal
448 cycles at TC 52 and seven cycles at TC 85. Even if at both TCs the mouth areas of some of
449 the largest tidal creeks were reached rapidly, a second tidal cycle appeared necessary for full
450 colonisation of the lateral dimension (inset in Figure 9). As mentioned above, this result did
451 not take into account that some further advancement in the creek could have eventually been
452 made during the high tide of the first tidal.

453 Successive tidal cycle modelling revealed the emergence of temporal connectivity
454 bottlenecks for weak dispersers. In particular, local connectivity disruptions behind the
455 colonisation front were observed at some stages of the flood in the first loop of the Seine
456 (Supplementary Figure S5). Fish that would have advanced above this area in the beginning
457 of the flood would remain in an area disconnected from downstream habitat patches at later
458 stages of the flood.

459 **Discussion**

460 The term “moving target“ has been coined in conservation biology to underline the
461 importance of considering habitat patch dynamics tracked by animal movement for
462 establishing meaningful measures of protection (Bull and others 2013). Highly dynamic
463 environments represent a challenge for understanding and quantifying patterns of habitat

464 availability, especially, because not only the structure (patch size and distribution), but also
465 functional connectivity of such landscapes varies in space and time (Zeigler and Fagan 2014).
466 Characterised by pronounced spatial dynamics of habitat turnover and connectivity at several
467 temporal scales, macrotidal estuaries are perfect examples of environments with constantly
468 “moving targets”.

469 Previous studies have mapped large-scale nursery availability (Nagelkerken and others
470 2015; Whaley and others 2007), and emphasised the paramount importance of the intra-
471 habitat connectivity for the value of estuarine and coastal nurseries (Secor and Rooker 2005;
472 Sheaves and others 2015). However, few have looked into the intra-tidal dynamics of the
473 estuarine habitat availability. Trapping and video observations during flood and ebb tides
474 recorded the transient habitat utilization by young stages of many necton species (Bretsch and
475 Allen 2006; Ellis and Bell 2008; Laffaille and others 2001). However, technically
476 challenging, such field studies are limited in spatial scale and temporal resolution. Spatio-
477 temporally explicit approaches, which integrate hydrological and biotic connectivity of a
478 landscape, appear indispensable for quantifying habitat dynamics and accessibility in large
479 estuaries. Our study represents, to our knowledge, the first case of least-cost modelling
480 application to estuarine habitats and the first example of investigating intra-tidal habitat
481 dynamics across a large estuary with such a fine spatio-temporal resolution.

482 Spatio-temporal bottlenecks in estuarine habitat availability and connectivity

483 In the pristine Seine estuary (large, shallow, and with weak lateral slopes), water level
484 increase during the tidal cycle must have led to a continuous shifting of shallow areas from
485 mudflats in the mouth area into tidal creeks and salt marshes (lateral shifts) as well as in the
486 upstream direction (longitudinal shifts). In these conditions, seabass juveniles probably had
487 access to nurseries throughout the tidal cycle and at any hydrological conditions. We observe

488 no spatio-temporally continuous access to shallow-water nurseries across the Seine estuary in
489 its current highly modified state. Altogether, we find a highly counter-intuitive result: the
490 relationship between water level and potential nursery surface availability is inversed. Thus,
491 in contrast to what we would expect in a pristine system, in the modern Seine estuary,
492 advancing tidal flow results in a dramatic drop of the total nursery habitat surface. This is
493 particularly pronounced on its south side, where temporary gaps in nursery distribution
494 emerge.

495 Highly modified topography of the Seine estuary is the most likely explanation for this
496 “surprise”, and this conclusion is in line with previous studies of artificialised floodplains of
497 the upstream Seine river (Le Pichon and others 2009) and the Saint-Lawrence River (Foubert
498 and others 2019). Harbour expansion, channel dredging, and creation of steep banks along
499 submersible dikes led to a massive loss of the intertidal zones (Cuvilliez and others 2009), and
500 introduced artificial « breaks » in the cross-sectional profile of the estuary (Supplementary
501 Figure S6). Consequently, in many areas of the mouth zone, no gradual transition between the
502 subtidal and the intertidal zones exists anymore. Instead, with the rising water level, shallow
503 patches get fragmented and small, and, at some point, disappear locally until a critical water
504 level allowing for dike submersion is reached, and the intertidal zones behind them become
505 available for colonisation. Dike construction and channel dredging have also modified the
506 estuarine permeability to movement. Our results show that flow velocities along the dikes
507 increase substantially during the tide. At some stages of the tide, channel current velocities are
508 so high that juvenile movement may only be possible in remaining narrow strips of slow flow
509 velocity along the channel margins.

510 The role of dispersal capacity for estuarine colonisation

511 In order to predict an organism's propagation through a landscape, we need to consider its
512 dispersal capacity and behaviour in interaction with the environment it encounters. In a
513 riverscape, the extent of fish movement is predominantly determined by the animal's
514 swimming capacity, the flow velocities, and the direction of the current. Behavioural
515 strategies of marine and estuarine fish, such as selective tidal transport, allow them to
516 augment movement range and reduce related energy costs in systems exposed to tides and
517 current reversal (Forward and Tankersley 2001). Here, testing several scenarios allowed us to
518 analyse the effects of swimming speed on the estuarine colonisation using selective tidal
519 transport. We show that, early juveniles with a low swimming capacity need several
520 successive tides to reach high-tide nurseries in the entire study area, while a single tide would
521 be sufficient by the end of their first summer.

522 Our results, representative of hydrological conditions at medium discharge ($250\text{m}^3.\text{s}^{-1}$)
523 ¹), suggest that colonisation is facilitated by low rather than by high TCs. On the occasion of
524 spring flooding, extreme river discharge levels (potential triggers of estuarine colonisation;
525 Jennings and Pawson 1992) may occur in the Seine estuary, whereby tidal flood current
526 velocities are counteracted by the river discharge (unpublished simulations of MARS-3D
527 model, Lemoine). This effect, which we, unfortunately, could not explore in the framework of
528 this study, should probably reduce both the speed of juvenile advancement in the estuary and
529 the extent of estuarine areas with high currents and thus the potential risk of being swept away
530 at high TCs.

531 Altogether, our comparison across different steps of the tidal cycle allows for several
532 conclusions. We show that transient local bottlenecks of nursery availability and accessibility
533 emerge in the Seine estuary during specific time windows of the tidal cycle. Our second
534 conclusion is that these bottlenecks are driven both by progressive habitat fragmentation and
535 by locally increasing riverscape resistance to movement. Finally, own mobility of juveniles

536 appears to play a key role for successful colonisation with weak dispersers obliged to follow a
537 stepping-stone-type colonisation.

538

539 Caveats and limitations of least-cost analysis

540 Chronological modelling approach, proposed here for dynamic environments, requires a
541 careful consideration of the choice of appropriate spatio-temporal scales. The latter should
542 cover the range of variation in both habitat availability and connectivity relevant for the
543 movement of the species with its specific ecological, behavioural and dispersal-related traits.
544 In the case of the seabass juvenile estuarine colonisation, the spatial component had to include
545 both an extent sufficient for covering the entire area of the estuarine mouth containing tidal
546 habitats, and a resolution allowing us to consider narrow tidal creeks and channel banks with
547 high-tide nurseries. Furthermore, the selection of time steps had to capture the structural
548 connectivity changes during the tidal cycle. Remote sensing data and a 2D-hydrodynamic
549 model available for the Seine estuary at high spatio-temporal resolution permitted us to fulfill
550 these criteria.

551 While our approach provides a highly flexible and spatially relevant framework, some
552 limitations related to biological assumptions and their translation into habitat and connectivity
553 modelling exist. Thus modelled nursery habitat was primarily defined by a combination of
554 water depth ranges and sediment characteristics established based on rare reported field
555 observations of juvenile seabass in the intertidal zones of NEA coast. Ideally, fine-scale field
556 investigations of nursery habitat characteristics, potentially taking into account further
557 dynamic variables (e.g. turbidity, temperature, dissolved oxygen or food availability) would
558 allow for a better delimitation of nursery habitats. Furthermore, in the connectivity analysis
559 applied we could not consider differences in habitat quality and patch size, which could affect
560 patch carrying capacity and juvenile preferences (Teichert and others 2018).

561 Parametrization of the least-cost analysis itself may also strongly affect its results.
562 Resistance values attributed to each pixel of a riverscape map are a crucial element linking
563 GIS-based data to the organism mobility and dispersal behaviour (Adriaensen and others
564 2003). Field or mesocosm studies quantifying the effect of high current velocities on early
565 juvenile fish could improve the calibration of riverscape resistance to movement and the
566 precision of the current velocity threshold above which water flow may become a barrier.
567 Further sensitivity analysis may allow for quantification of the effects of these parameters and
568 the related error margins (Beier and others 2008). However, in the case of complex
569 chronological calculations as the ones presented here, investigating ranges of values is rapidly
570 translated into long computation times and a compromise needs to be found. Here we chose to
571 focus on testing a plausible range of juvenile seabass mobility parameters.

572 Implications for management and conservation

573 Fish stocks of many marine and estuarine species experience a drastic decline (Christensen
574 and others 2014; Vasilakopoulos and others 2014). Increasing attention has been given in the
575 last decades to identifying population bottlenecks, notably at the sensitive stages of spawning,
576 juvenile colonisation of nurseries and growth, to be targeted by management and conservation
577 efforts (Sheaves and others 2015). In macrotidal estuaries, the nature and drivers of such
578 bottlenecks may be difficult to identify and common-sense assumptions (as simple as “higher
579 water level means more available intertidal habitat”) may prove to be misleading in human-
580 modified systems.

581 Chronological functional connectivity modelling offers a road for addressing this
582 challenge. Zooming into the processes occurring during tidal cycles helps disentangle the
583 effects of habitat fragmentation and riverscape connectivity and identify the timing of
584 occurrence and location of the transient bottlenecks that may affect habitat colonisation by

585 juveniles. Maps produced by our approach may be directly used to test and visualize the
586 consequences of different management scenarios, and subsequently guide decision-making
587 (e.g. prioritisation of areas for dike removal or for conservation).

588 Our work demonstrates that focusing exclusively on the protection and restoration of
589 high tide nurseries may prove inefficient, as they may be disconnected from the succession of
590 habitat patches needed over the tidal cycle. This is an empirical illustration to the notions of
591 “moving targets” (Bull and others 2013), “seascape nurseries” (mosaics of functionally
592 connected habitat patches; Nagelkerken and others 2015) and “transient windows for
593 connectivity” (Zeigler and Fagan 2014) formulated in conservation biology and emphasising
594 the importance of taking the mobile nature of connectivity and habitats into account when
595 planning conservation measures. We suggest that chronological functional connectivity
596 modelling is a valuable tool applicable to any ecosystem where organisms have to cope with
597 highly dynamic environments over their life cycle.

598

599 **Acknowledgments**

600 This study has been carried out in the framework of the ANACONDHA project funded by the
601 scientific research program of the GIP Seine-Aval. We cordially thank Nicolas Bacq for his
602 invaluable support, ideas and work orientations throughout the project, Sylvain Duhamel, Eric
603 Feunteun, Ronan Le Goff, Mike Pawson, H el ene de Pontual, Florian Rozanska and St ephanie
604 Moussard for sharing their expertise and time during fruitful discussions at different stages of
605 this project, Jean-Philippe Lemoine for producing MARS-3D model outputs, Eric L’Ebreillec
606 for preparing habitat and water depth maps and providing supplementary data on the Seine
607 estuary, Sylvain Descloux for his support with improving ANAQUALAND, and Amandine
608 Zahm for running part of the tested scenarios. We kindly thank two anonymous reviewers and

609 the editors for their very constructive and insightful comments that helped to substantially
610 improve the manuscript throughout the revision process.

611 **References**

- 612 Adriaensen F, Chardon JP, De Blust G, Swinnen E, Villalba S, Gulinck H, Matthysen E. 2003.
613 The application of 'least-cost' modelling as a functional landscape model. *Landsc Urb*
614 *Plan* 64:233-247.
- 615 Avoine J, Allen GP, Nichols M, Salomon JC, Larssonneur C. 1981. Suspended-sediment
616 transport in the Seine estuary, France: Effect of man-made modifications on estuary—
617 shelf sedimentology. *Mar Geol* 40:119-137.
- 618 Baguette M, Blanchet S, Legrand D, Stevens VM, Turlure C. 2013. Individual dispersal,
619 landscape connectivity and ecological networks. *Biol Rev* 88:310-326.
- 620 Beier P, Majka DR, Spencer WD. 2008. Forks in the road: choices in procedures for designing
621 wildland linkages. *Conserv Biol* 22:836-851.
- 622 Bretsch K, Allen DM. 2006. Tidal migrations of nekton in salt marsh intertidal creeks.
623 *Estuaries Coast* 29:474-486.
- 624 Bull JW, Suttle KB, Singh NJ, Milner-Gulland E. 2013. Conservation when nothing stands
625 still: moving targets and biodiversity offsets. *Front Ecol Environ* 11:203-210.
- 626 Cabral H, Costa MJ. 2001. Abundance, feeding ecology and growth of 0-group sea bass,
627 *Dicentrarchus labrax*, within the nursery areas of the Tagus estuary. *J Mar Biol Assoc*
628 *UK* 81: 679-682.
- 629 Caldwell I, Gergel S. 2013. Thresholds in seascape connectivity: influence of mobility,
630 habitat distribution, and current strength on fish movement. *Landsc Ecol* 28:1937-1948.
- 631 Capra H, Plichard L, Bergé J, Pella H, Ovidio M, McNeil E, Lamouroux N. 2017. Fish habitat
632 selection in a large hydropeaking river: Strong individual and temporal variations
633 revealed by telemetry. *Sci Tot Environ* 578:109-120.
- 634 Carbonneau P, Piégay H. 2012. Fluvial remote sensing for science and management. John
635 Wiley & Sons.

636 Cattrijsse A, Makwaia ES, Dankwa HR, Hamerlynck O, Hemminga MA. 1994. Nekton
637 communities of an intertidal creek of a European estuarine brackish marsh. *Mar Ecol*
638 *Progr Ser* 109: 195-208.

639 Cattrijsse A, Hampel H. 2006. European intertidal marshes: a review of their habitat
640 functioning and value for aquatic organisms. *Mar Ecol Prog Ser* 324: 293-307.

641 Christensen V, Coll M, Piroddi C, Steenbeek J, Buszowski J, Pauly D. 2014. A century of
642 fish biomass decline in the ocean. *Mar Ecol Prog Ser* 512: 155-166.

643 Claireaux G, Couturier C, Groison A-L. 2006. Effect of temperature on maximum swimming
644 speed and cost of transport in juvenile European sea bass (*Dicentrarchus labrax*). *J Exp*
645 *Biol* 209:3420-3428.

646 Cuvilliez A, Deloffre J, Lafite R, Bessineton C. 2009. Morphological responses of an
647 estuarine intertidal mudflat to constructions since 1978 to 2005: The Seine estuary
648 (France). *Geomorphology* 104:165-174.

649 Ellis WL, Bell SS. 2008. Tidal influence on a fringing mangrove intertidal fish community as
650 observed by in situ video recording: implications for studies of tidally migrating nekton.
651 *Mar Ecol Prog Ser* 370:207-219.

652 Fahrig L. 1992. Relative importance of spatial and temporal scales in a patchy environment.
653 *Theor Popul Biol* 41:300-314.

654 Forward RB, Tankersley RA. 2001. Selective tidal-stream transport of marine animals.
655 *Oceanogr Mar Biol* 39:305-353.

656 Foubert A, Le Pichon C, Mingelbier M, Farrell JM, Morin J, Lecomte F. 2019. Modeling the
657 effective spawning and nursery habitats of northern pike within a large spatiotemporally
658 variable river landscape (St. Lawrence River, Canada). *Limnol Oceanogr* 64:803-819.

659 Foussard V, Cuvilliez A, Fajon P, Fisson C, Lesueur P, Macur O. 2010. Evolution
660 morphologique d'un estuaire anthropisé de 1800 à nos jours. Fascicule Seine-Aval 2.3.
661 <https://www.seine-aval.fr/publication/fasc-evolution-morphologique/>

662 Fritsch M. 2005. Traits biologiques et exploitation du bar commun *Dicentrarchus labrax* (L.)
663 dans les pêcheries françaises de la manche et du golfe de Gascogne. Doctoral
664 dissertation, University of Western Brittany.

665 Gibson RN. 2003. Go with the flow: tidal migration in marine animals. *Hydrobiologia*
666 503:153-161.

667 Grasso F, Le Hir P. 2019. Influence of morphological changes on suspended sediment
668 dynamics in a macrotidal estuary: diachronic analysis in the Seine Estuary (France)
669 from 1960 to 2010. *Ocean Dyn* 69:83-100.

670 Green BC, Smith DJ, Grey J, Underwood GJ. 2012. High site fidelity and low site
671 connectivity in temperate salt marsh fish populations: a stable isotope approach.
672 *Oecologia* 168:245-255.

673 Hanke MH, Lambert JD, Smith KJ. 2014 Utilization of a multicriteria least-cost path model
674 in an aquatic environment. *Int J Geogr Inf Sci* 28:1642-1657.

675 Hohensinner S, Jungwirth M, Muhar S, Schmutz S. 2011. Spatio-temporal habitat dynamics
676 in a changing Danube River landscape 1812-2006. *Riv Res Appl* 27:939-955.

677 Jennings S, Lancaster JE, Ryland JS, Shackley SE. 1991. The age structure and growth
678 dynamics of young-of-the-year bass, *Dicentrarchus labrax*, populations. *J Mar Biol*
679 *Assoc UK* 71:799-810.

680 Jennings S, Pawson M. 1992. The origin and recruitment of bass, *Dicentrarchus labrax*,
681 larvae to nursery areas. *J Mar Biol Assoc UK* 72:199-212.

682 Kelley D. 1986. Bass nurseries on the west coast of the UK. *J Mar Biol Assoc UK* 66: 439-
683 464.

684 Kelley D. 2002. Abundance, growth and first-winter survival of young bass in nurseries of
685 south-west England. *J Mar Biol Assoc UK* 82:307-19.

686 Keymer JE, Marquet PA, Velasco-Hernández JX, Levin SA. 2000. Extinction thresholds and
687 metapopulation persistence in dynamic landscapes. *Am Nat* 156:478-494.

688 Laffaille P, Lefeuvre J-C, Schricke M-T, Feunteun E. 2001. Feeding ecology of o-group sea
689 bass, *Dicentrarchus labrax*, in salt marshes of Mont Saint Michel Bay (France).
690 *Estuaries* 24:116-125.

691 Lafite R, Romaña L-A. 2001. A man-altered macrotidal estuary: the Seine estuary (France):
692 introduction to the special issue. *Estuaries Coast* 24:939-939.

693 Le Hir P, Lafite R. 2012. Projet MODEL: Modélisation validée de l'hydro-morpho-
694 sédimentologie, base physique d'une modélisation environnementale de l'estuaire de la
695 Seine. GIP Seine Aval <https://www.seine-aval.fr/projet/model/>

696 Le Pichon C, Gorges G, Baudry J, Goreaud F, Boët P. 2009. Spatial metrics and methods for
697 riverscapes: quantifying variability in riverine fish habitat patterns. *Environmetrics*
698 20:512-526.

699 Le Pichon C, Gorges G, Faure T, Boussard H. 2006. Anaqualand 2.0: freeware of distances
700 calculations with frictions on a corridor. 2.0 edn. Cemagref, Antony
701 <https://www6.rennes.inra.fr/sad/Outils-Produits/Outils-informatiques/Anaqualand>.

702 Leis JM, Balma P, Ricoux R, Galzin R. 2012. Ontogeny of swimming ability in the European
703 sea bass, *Dicentrarchus labrax* (L.)(Teleostei: Moronidae) *Mar Biol Re.* 8:265-72.

704 Lesourd S, Lesueur P, Fisson C, Dauvin J-C. 2016. Sediment evolution in the mouth of the
705 Seine estuary (France): A long-term monitoring during the last 150 years. *CR Geosci*
706 348:442-450.

707 López R, de Pontual H, Bertignac M, Mahévas S. 2015. What can exploratory modelling tell
708 us about the ecobiology of European sea bass (*Dicentrarchus labrax*): a comprehensive
709 overview. *Aquat Living Resour* 28:61-79.

710 Lotze HK, Lenihan HS, Bourque BJ, Bradbury RH, Cooke RG, Kay MC, Kidwell SM, Kirby,
711 MX, Peterson CH, Jackson JBC. 2006. Depletion, degradation, and recovery potential
712 of estuaries and coastal seas. *Science*, 312:1806-1809.

713 Martinho F, Leitão R, Neto JM, Cabral H, Lagardère F, Pardal MA. 2008. Estuarine
714 colonization, population structure and nursery functioning for 0-group sea bass
715 (*Dicentrarchus labrax*), flounder (*Platichthys flesus*) and sole (*Solea solea*) in a
716 mesotidal temperate estuary. *J App Ichthyol* 24:229-237.

717 Nagelkerken I, Sheaves M, Baker R, Connolly RM. 2015. The seascape nursery: a novel
718 spatial approach to identify and manage nurseries for coastal marine fauna. *Fish Fish*
719 16:362-371.

720 Neumann W, Martinuzzi S, Estes AB, Pidgeon AM, Dettki H, Ericsson G, Radeloff VC. 2015.
721 Opportunities for the application of advanced remotely-sensed data in ecological studies
722 of terrestrial animal movement. *Mov Ecol* 3:8.

723 Pastoureaud A. 1991. Influence of starvation at low temperatures on utilization of energy
724 reserves, appetite recovery and growth character in sea bass, *Dicentrarchus labrax*.
725 *Aquac* 99:167-178.

726 Pickett GD, Pawson MG. 1994. Sea bass. Biology, exploitation and conservation. Chapman
727 & Hall.

728 Ray N, Lehmann A, Joly P. 2002. Modeling spatial distribution of amphibian populations: a
729 GIS approach based on habitat matrix permeability. *Biodivers Conserv* 11:2143-2165.

730 Rochette S, Rivot E, Morin J, Mackinson S, Riou P, Le Pape O. 2010. Effect of nursery habitat
731 degradation on flatfish population: Application to *Solea solea* in the Eastern Channel
732 (Western Europe). J Sea Res 64:34-44.

733 Rouget M, Cowling RM, Lombard AT, Knight AT, Kerley GIH. 2006. Designing large-scale
734 conservation corridors for pattern and process. Conserv Biol 20:549-561.

735 Rountree RA, Able KW. 2007. Spatial and temporal habitat use patterns for salt marsh nekton:
736 implications for ecological functions. Aquat Ecol 41:25-45.

737 Roy ML, Le Pichon C. 2017. Modelling functional fish habitat connectivity in rivers: A case
738 study for prioritizing restoration actions targeting brown trout. Aquat Conserv 27:927-
739 937.

740 Schlosser IJ. 1995. Critical landscape attributes that influence fish population dynamics in
741 headwater streams. Hydrobiologia 303:71-81.

742 Secor H, Rooker JR. 2005. Connectivity in the life histories of fishes that use estuaries. Estuar
743 Coast Shelf Sci 64:1-3.

744 Selleslagh J, Amara R. 2008. Environmental factors structuring fish composition and
745 assemblages in a small macrotidal estuary (eastern English Channel). Estuar Coast Shelf
746 Sci 79:507-517.

747 Sheaves M. 2009. Consequences of ecological connectivity: the coastal ecosystem mosaic.
748 Mat Ecol Prog Ser 391:107-115.

749 Sheaves M, Baker R, Nagelkerken I, Connolly RM. 2015. True value of estuarine and coastal
750 nurseries for fish: incorporating complexity and dynamics. Estuaries Coast 38:401-414.

751 Stanford JA, Lorang MS, Hauer FR. 2005. The shifting habitat mosaic of river ecosystems.
752 SIL Proc 29:123-136;

753 Sutcliffe OL, Bakkestuen V, Fry G, Stabbetorp OE. 2003. Modelling the benefits of farmland
754 restoration: methodology and application to butterfly movement. *Landsc Urban Plan*
755 63:15-31.

756 Taylor PD, Fahrig L, Henein K, Merriam G. 1993. Connectivity is a vital element of landscape
757 structure. *Oikos* 68:571-573.

758 Tecchio S, Chaalali A, Raoux A, Tous Rius A, Lequesne J, Girardin V, Lassalle G, Cachera
759 M, Riou P, Lobry J, Dauvin J-C, Niquil N. 2016. Evaluating ecosystem-level
760 anthropogenic impacts in a stressed transitional environment: The case of the Seine
761 estuary. *Ecol Indic* 61:833-845.

762 Teichert N, Carassou L, Sahraoui Y, Lobry J, Lepage M. 2018. Influence of intertidal
763 seascape on the functional structure of fish assemblages: Implications for habitat
764 conservation in estuarine ecosystems. *Aquat Conserv* 28:798-809.

765 Tonolla D, Acuña V, Uehlinger U, Frank T, Tockner K. 2010. Thermal heterogeneity in river
766 floodplains. *Ecosyst* 13:727-740.

767 Vasilakopoulos P., Maravelias CD, Tserpes G. 2014. The alarming decline of Mediterranean
768 fish stocks. *Curr Biol*, 24: 1643-1648.

769 Whaley SD, Burd Jr JJ, Robertson BA. 2007. Using estuarine landscape structure to model
770 distribution patterns in nekton communities and in juveniles of fishery species. *Mar*
771 *Ecol Progr Ser* 330:83-99.

772 Wiens JA. 1976. Population responses to patchy environments. *Ann Rev Ecol Syst* 7:81-120.

773 Wimberly MC. 2006. Species dynamics in disturbed landscapes: when does a shifting habitat
774 mosaic enhance connectivity? *Landsc Ecol* 21: 35-46.

775 Zeigler SL, Fagan WF. 2014. Transient windows for connectivity in a changing world. *Mov*
776 *Ecol* 2:1.

777 Zeller KA, McGarigal K, Whiteley AR. 2012. Estimating landscape resistance to movement:
778 a review. *Landsc Ecol* 27:777-797.

779 **Figure captions**

780 **Figure 1:** A life cycle example (inspired by Schlosser 1995) with (a) living space (all
781 habitats) occupied by each stage; (b) example of directed daily movements (e.g. tidal
782 dynamics) of a single stage between habitats; (c) seasonal dynamics of habitat use of another
783 life stage (adult). $t_N \dots t_{N+i}$ represent points in time, whereby time scales may vary.

784

785 **Figure 2:** The spatial extent of the Seine estuary considered in this study. High-tide wetted
786 area at TC 85 (at $250 \text{ m}^3 \text{ s}^{-1}$) is presented for 2010. Historical estuarine data is based on the
787 maps of Magin and Magin (1750).

788

789 **Figure 3:** Time-step-specific resistance maps used for modelling upstream movement of
790 juveniles with the flood (two TCs and discharge of $250 \text{ m}^3 \text{ s}^{-1}$). Colours represent resistance
791 values (R) calculated based on mean current velocities (V).

792

793 **Figure 4:** The principle of habitat patch connectivity calculation between tidal time steps.
794 $H(t_N)$ represents departure habitat at time point t_N ; $H(t_{N+1})$ represent patches of potentially
795 available habitat at the next time point t_{N+1} . The dotted lines delineate the areas within
796 threshold functional distances calculated with the least-cost modelling for four hypothetical
797 scenarios. In scenario 4, only the part of $H(t_{N+1})$ in light grey is connected to $H(t_N)$ and
798 retained for the next step of the analysis.

799

800 **Figure 5:** Intra-annual analysis: high-tide nursery surface areas at four TCs and two levels of
801 discharge on the north and south side: a) total potential nursery area; b) potential nursery area
802 by estuarine sector.

803

804 **Figure 6:** Distribution of nursery habitats in the beginning and at the end of the flood at two
805 TCs and discharge of $250 \text{ m}^3 \text{ s}^{-1}$.

806

807 **Figure 7:** Nursery surface change during the flood at two TCs and discharge of $250 \text{ m}^3 \text{ s}^{-1}$: a)
808 total potential nursery area; b) potential nursery area by estuarine sector.

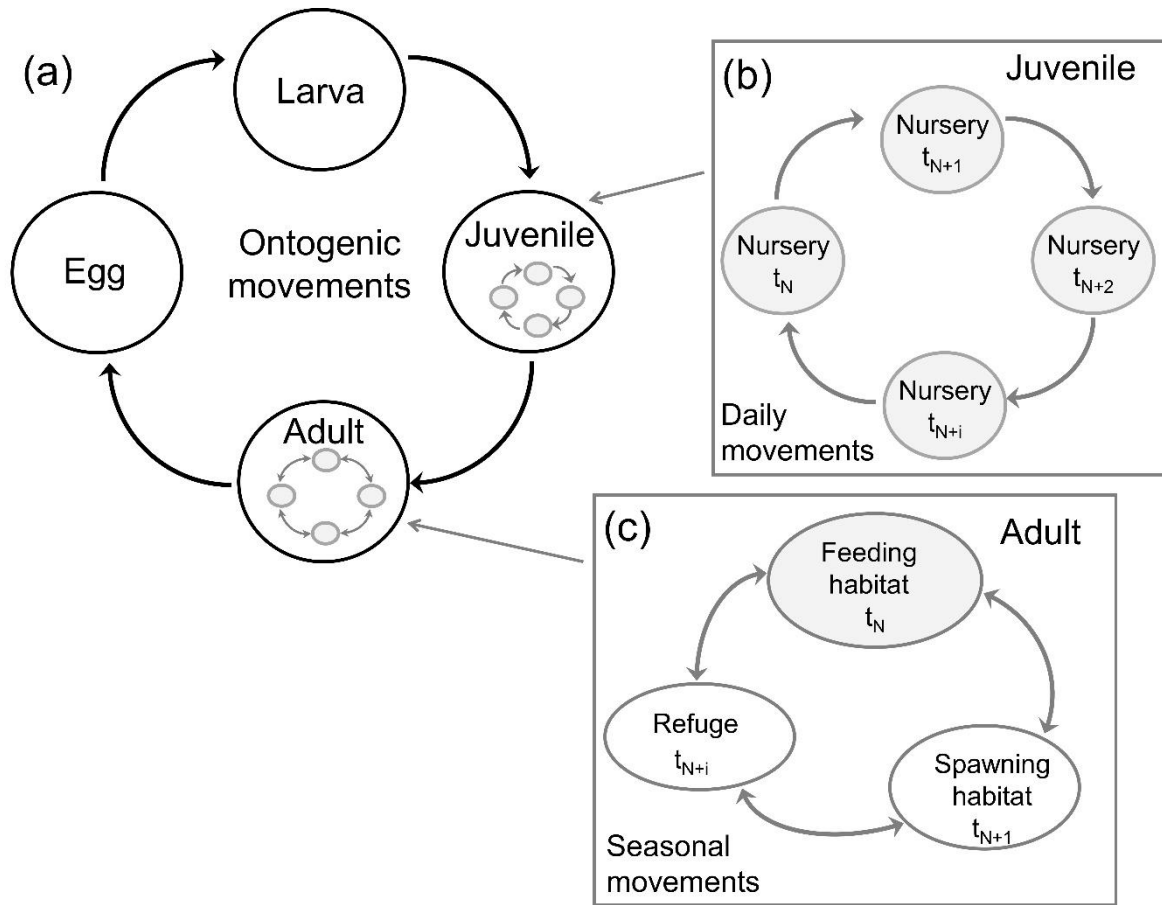
809

810 **Figure 8:** Colonisation front under different swimming speed scenarios at two TCs and
811 discharge of $250 \text{ m}^3 \text{ s}^{-1}$. Separate arrows are shown for the south and the north, when
812 colonisation fronts on the two sides are not aligned.

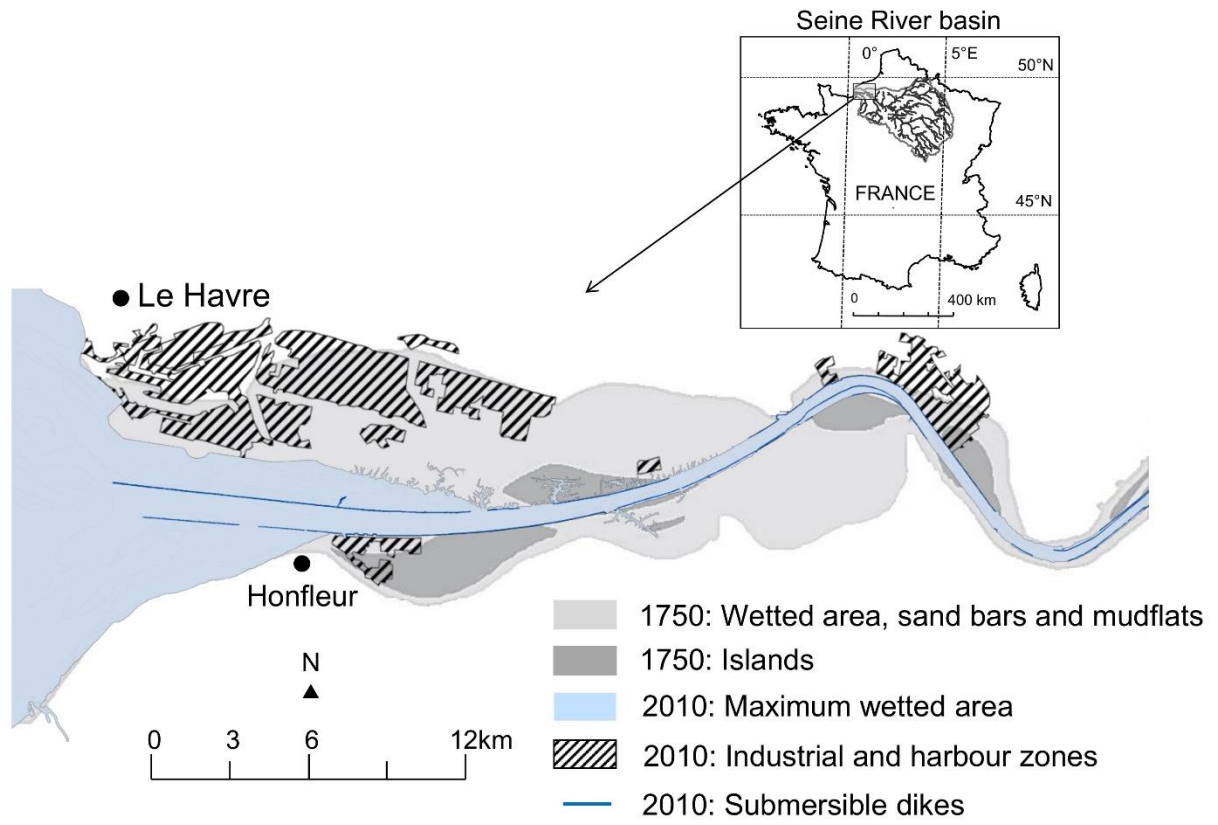
813

814 **Figure 9:** Successive tidal colonisation fronts modelled at two TCs and discharge of $250 \text{ m}^3 \text{ s}^{-1}$
815 ¹ for the 0.05 m s^{-1} swimming speed scenario. The inset (b) shows details of the lateral
816 intertidal zones colonised at TC 52 with the first tide. Separate arrows are shown for the south
817 and the north, when colonisation fronts on the two sides are not aligned.

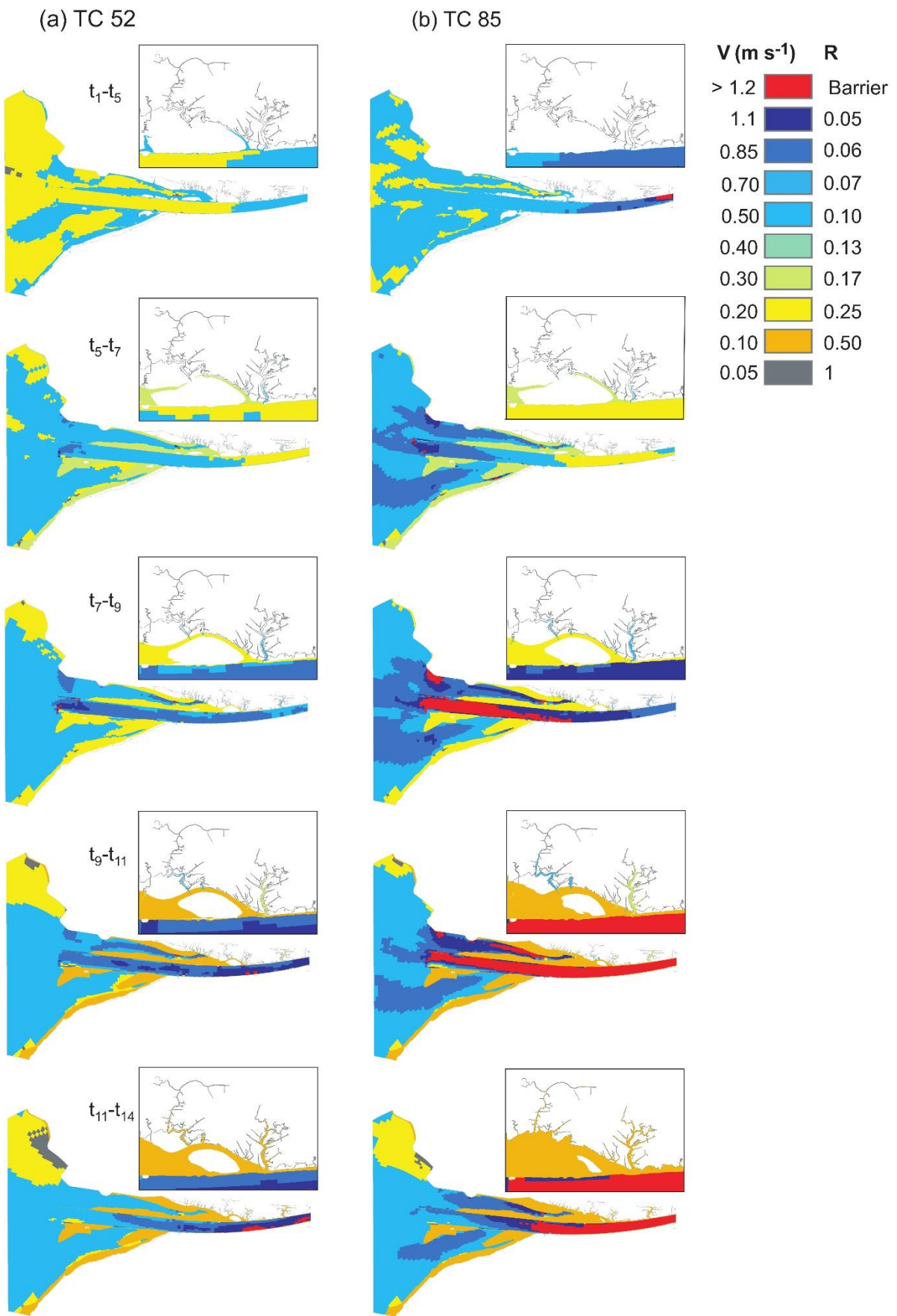
818 **Figures**
819
820 **Figure 1**



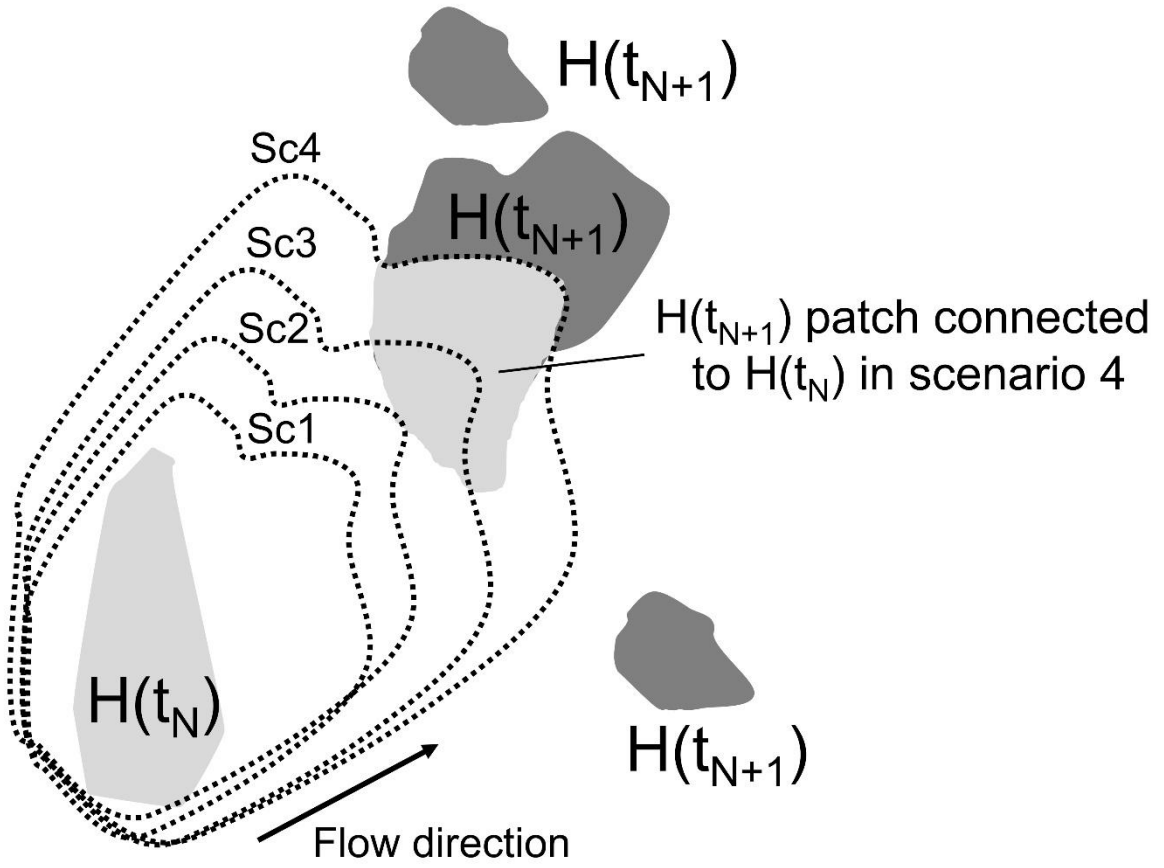
822
823



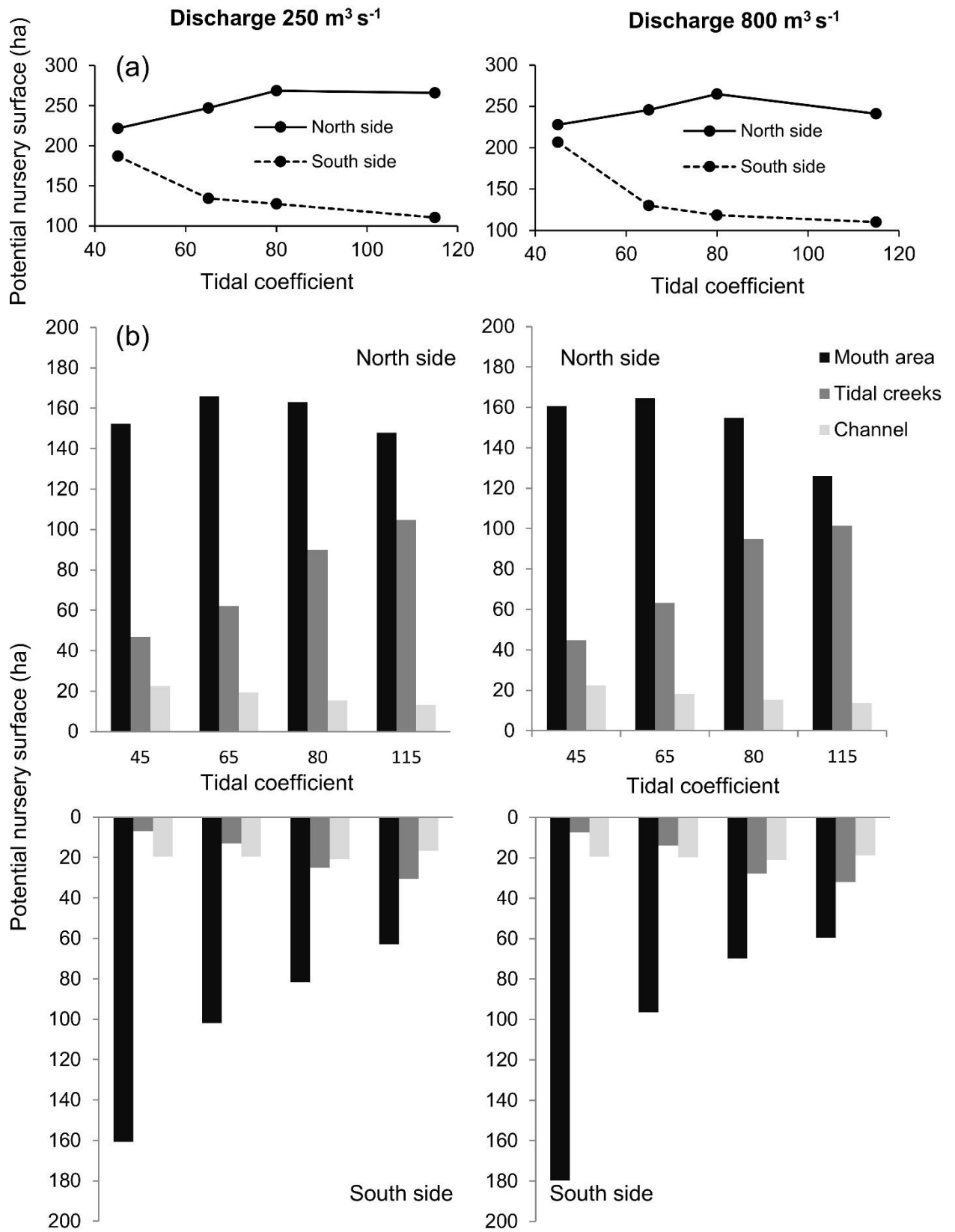
825
826



829 **Figure 4**

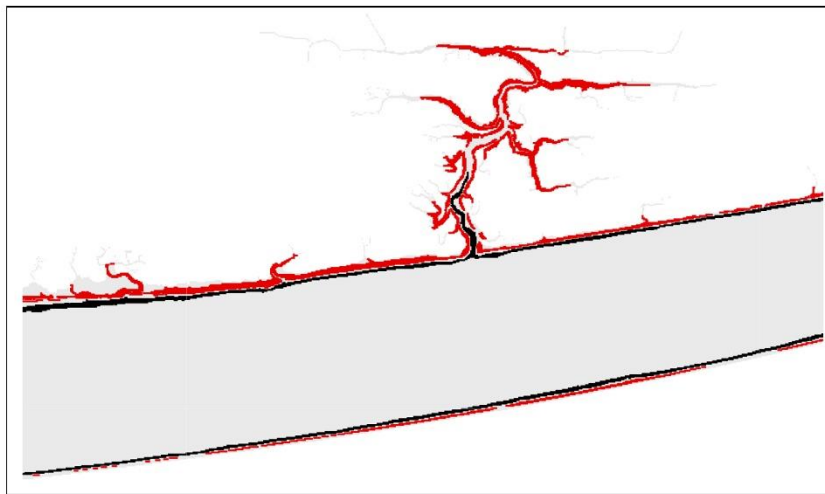
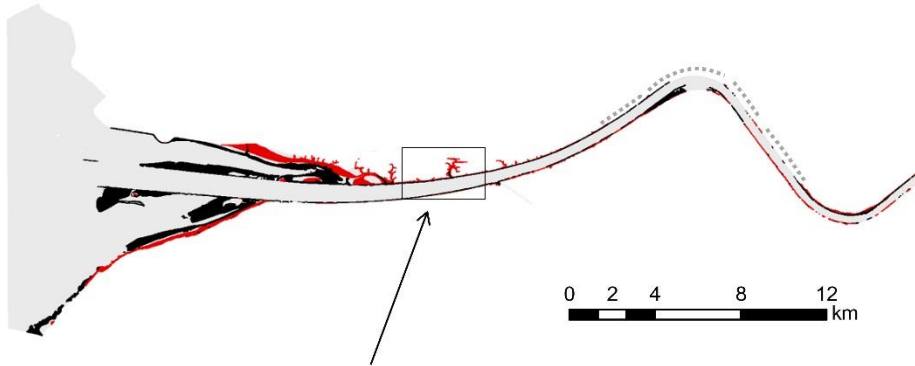


830
831
832

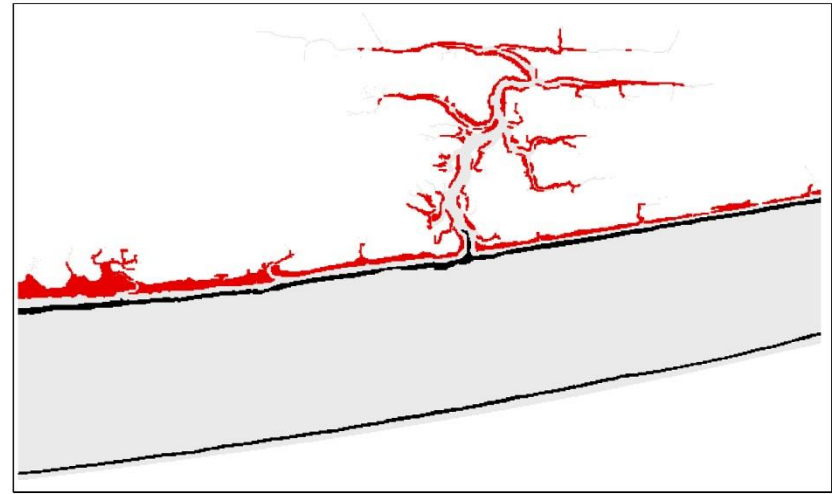
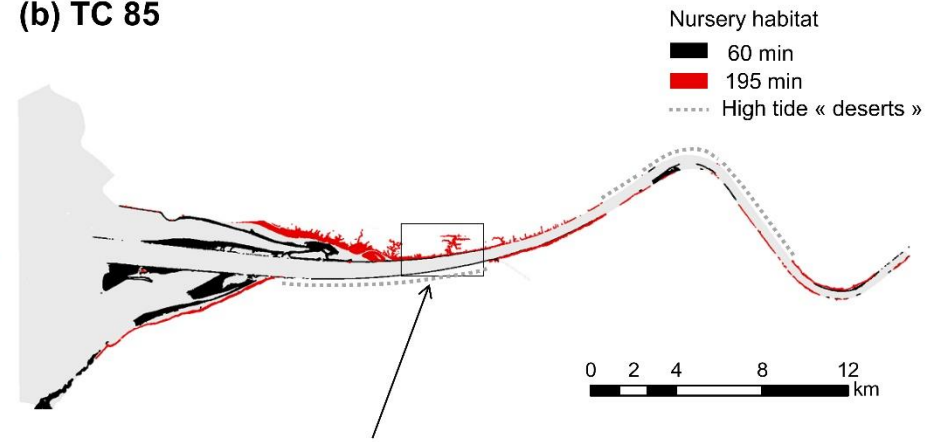


836 **Figure 6**

(a) TC 52



(b) TC 85



837
838
839

Figure 7

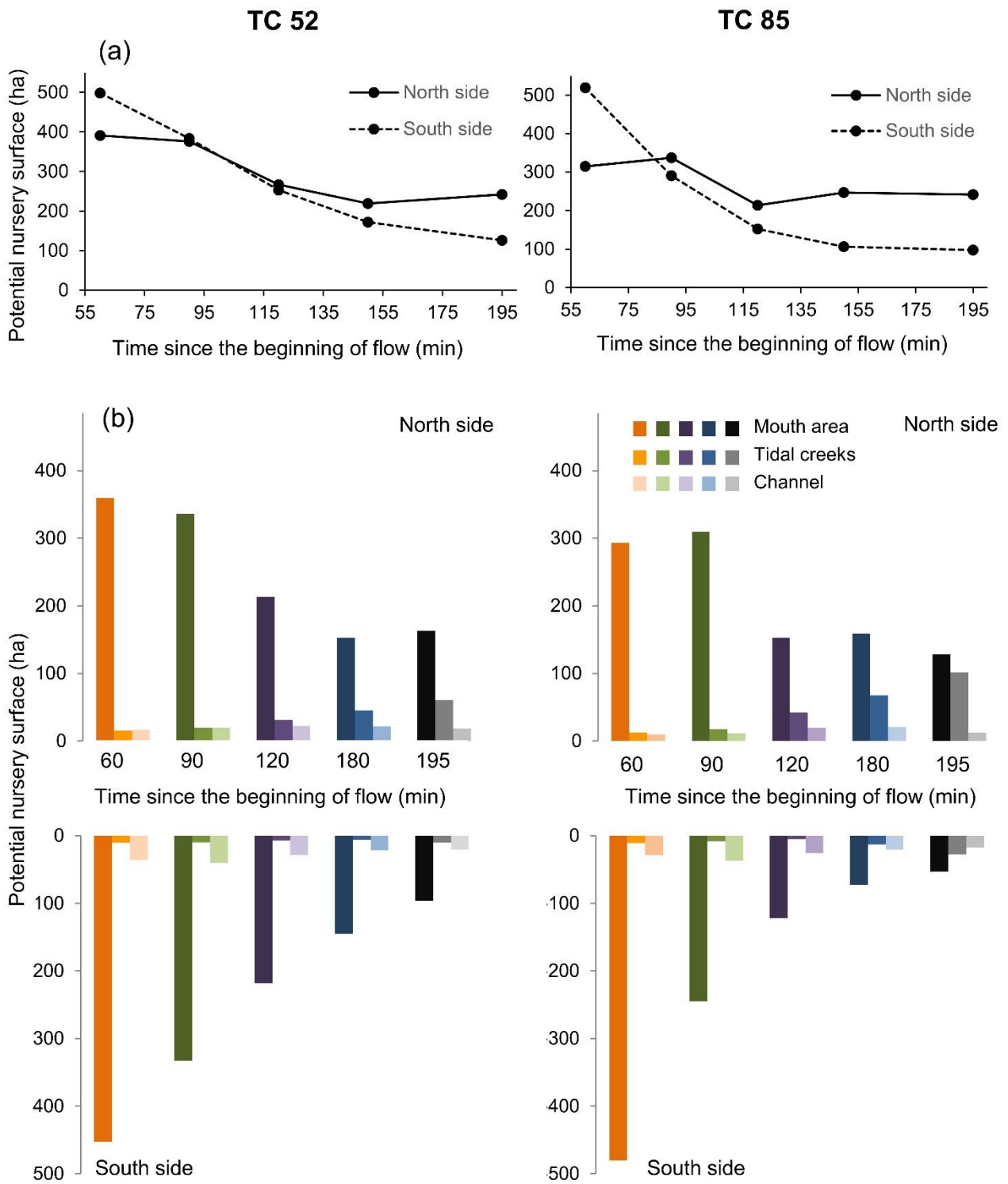


Figure 8

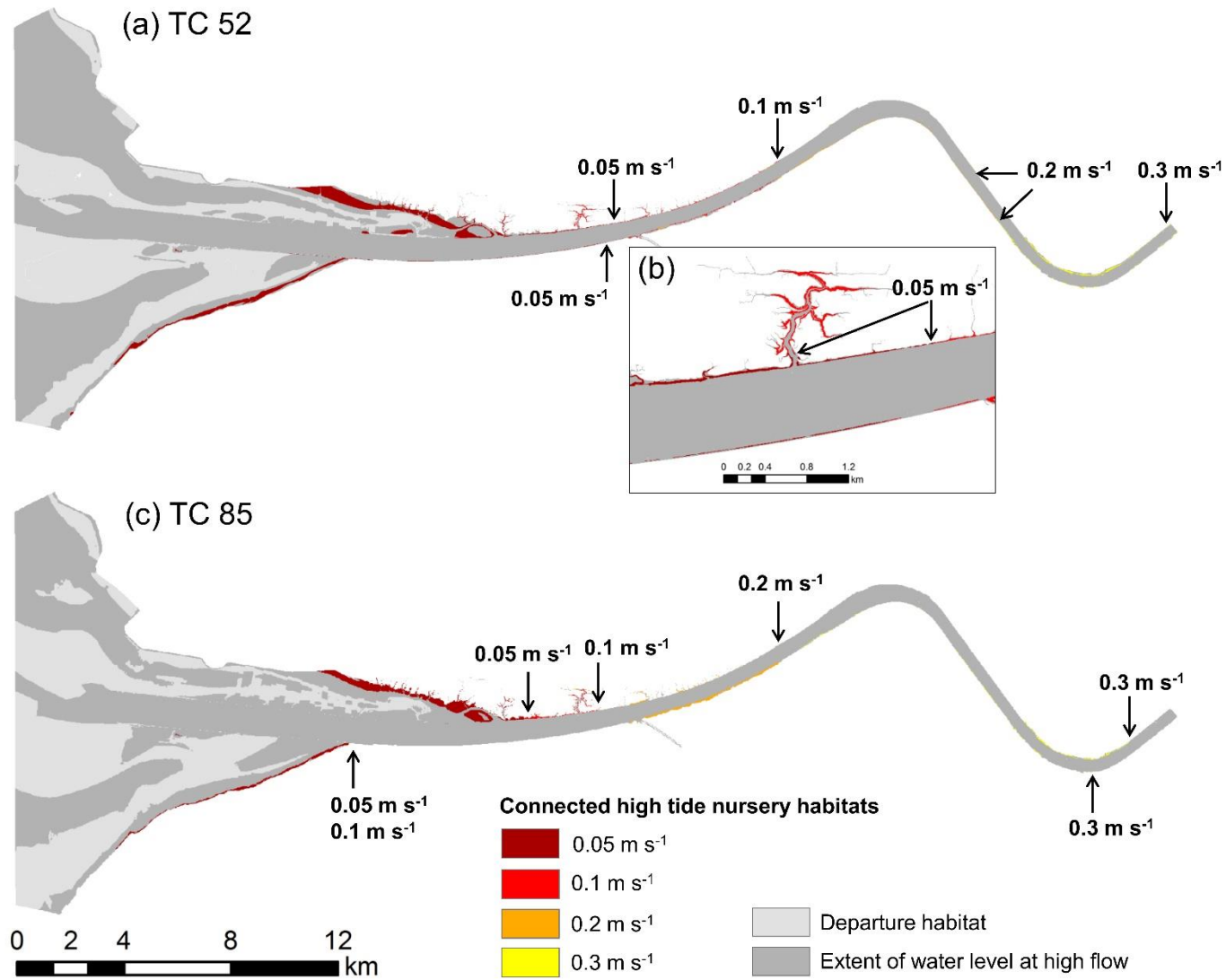


Figure 9

